SPACECRAFT RADIATOR PROTECTION FROM IONIZING RADIATION, DUST, AND EXCESSIVE HEAT LOSS

Vijay V. Devarakonda and Michael D. Hogue
Analytical Scientific Products LLC

Darnell Cowan
NASA JSC

ABSTRACT

Under a NASA Phase II SBIR project (Contract No. 80NSSC25C0088), Analytical Scientific Products (ASP) has been developing an actively controlled louver to protect spacecraft radiators from degradation due to exposure to various types of environmental conditions. Of particular interest are ionizing radiation during spacecraft transit through the Van Allen belts, dust during lunar landing and surface operations, and excessive heat loss during the long lunar night especially near the poles where the local temperatures can drop below -200°C. Exposure to ionizing radiation and dust can degrade the optical properties of the radiator coating that reduces its ability to reject excess heat from the spacecraft into the environment. Exposure to the extremely cold lunar night conditions near the poles can freeze the heat transfer fluids that can compromise the integrity of the radiator. Passive louvers constructed using relatively thick aluminum vanes are used currently to protect spacecraft radiators from some of the above effects, but they have several drawbacks: (i) their high aerial density makes it impractical to scale them to protect the much larger spacecraft radiators needed for future manned missions to the moon and beyond, (ii) passive louvers rely on bimetallic actuators to open and close the vanes that are controlled solely by external temperatures, and as a result the passive louvers cannot protect the radiators from dust and ionizing radiation when the ambient temperatures are high, (iii) the bimetallic actuators need time scales of the order of hours to open and close, and (iv) passive louvers are built from aluminum that provides only minimal protection against the ionizing radiation in Van Allen belts.

We have addressed the above limitations of passive louvers through the development of a low aerial density and rapidly actuating actively controlled louver. It is constructed from a custom alloy that offers much higher levels of protection against the ionizing radiation, dust and excessive heat loss at a fraction of weight compared to passive louvers while providing opening and closing time scales of the order of a second. Our modular design makes it easy to scale the system up or down depending on the application. We have recently constructed a 31 inch × 31 inch module of this louver and tested its functionality and performance. These tests have shown that the louver vanes can be opened and closed in less than a second. It reduces the transmission of ionizing radiation by 57% to 100% (depending on the radiation source), dust transmission by more than 93%, and heat loss by more than 97%. We are currently preparing to evaluate this device inside a cryogenic vacuum chamber where it can be subjected to simulated lunar surface conditions. This paper provides a detailed discussion of the test systems and the test data that demonstrate the effectiveness of our louver in reducing the transmission of ionizing radiation, dust, and heat under laboratory conditions.

Trade names and trademarks are used in this report for identification only. Their usage does not constitute an official endorsement, either expressed or implied, by the National Aeronautics and Space Administration.

INTRODUCTION

There is a strong interest in developing the infrastructure needed to enable sustaining human presence on the moon as part of the Artemis program. Current lunar orbit and surface habitat concepts incorporate conventional single-phase radiators coated with the highly radiative Z-93 to reject heat. These habitats will be exposed to high energy and ionizing radiation while traveling through the Van Allen belts that can last from hours to days. Previous studies conducted by NASA have shown that exposure to >500 equivalent sun hours (ESH) in the Van Allen belts can increase the radiator's Z-93 absorptivity from 0.16 to 0.24, or 50%, that can lower its heat rejection capability significantly. On the moon, the radiators will be exposed to elevated levels of the highly adhesive lunar dust that can easily coat the radiator's surface degrading its optical properties. Tests conducted by NASA have shown that Z-93 absorptivity degrades linearly with the amount of dust coverage on the coating. As little as 20% dust coverage can increase the absorptivity by 75% decreasing the heat rejection capability considerably. Habitats stationed near the lunar south pole will be exposed to temperatures as low as -213°C (or -351°F) during lunar nights that can last up to 14 days. These temperatures are below the freezing point of heritage or candidate active thermal control system coolants like ammonia, water, Freon, and HFE 7200. Conservation of energy analysis revealed that large amounts of heater power (up to 4 kW) is required to prevent freezing of heritage coolants and maintain safe operations [1-5].

NASA considered solving the above issues by placing the radiators behind passive louvers that are opened and closed by bimetallic springs which respond passively to the radiator temperature [6]. The passive louvers have several drawbacks including: (i) very long actuation times of the order of 1 – 2 hours that are too slow for this application, (ii) large mass penalties (up to 1 kg to shield 0.14 m^2 area) due to the use of relatively thick louver vanes (few mm) that make them impractical for scaleup to protect large radiators needed for future manned spacecraft to the moon and other planetary bodies, (iii) inability to effectively block radiation and dust even when the louvers are in closed position, (iv) reductions in radiator efficiency by 7 to 13% when the louver vanes are completely open, (v) limited effectiveness in protecting the radiator from excessive heat loss during the lunar night near the poles, and (vi) potential for solar entrapment that reduces the radiator's ability to reject excess heat generated in the spacecraft.

ACTIVELY CONTROLLED LOUVER TECHNOLOGY

Analytical Scientific Products (ASP) has been developing a lightweight and fast actuating actively controlled louver to protect spacecraft radiators from performance degradation due to ionizing radiation, dust, excessive heat loss, and solar entrapment. In Phase I of this SBIR project, we have designed, constructed and evaluated the feasibility of a 0.14 m^2 louver. In Phase II, we have designed a modular 7 m^2 device that consists of 12 modules arranged in 3 stacks. Each module has a height of 31 inches and a width of 31 inches and is built from 6 individual vanes whose opening and closing are synchronized. A single compact, lightweight and low power motor is used to control the opening and closing of all the vanes in the 12 modules. This louver is constructed using an alloy that has been optimized to provide high level of attenuation from the ionizing radiation expected during transit through the Van Allen belts. The high attenuation coefficient of this material enabled us to reduce the vane thickness significantly which in turn reduced the aerial density and the mass of the overall device. Our louver vanes also have very low thermal emissivity

Trade names and trademarks are used in this report for identification only. Their usage does not constitute an official endorsement, either expressed or implied, by the National Aeronautics and Space Administration.

and absorptivity that reduce the heat loss from the radiator during the cold lunar night. Our low power and lightweight motor is designed to open/close the louver vanes in seconds. Moreover, since the vane opening and closing is controlled actively, our technology offers the additional benefit of opening/closing the vanes partially, if needed. The partial opening can be an effective approach to reduce the solar radiation that can reach the radiator during routine operation. It can also help mitigate the effects of dust from a nearby lunar surface operation while the radiator is rejecting heat to the environment. As a part of this project, we have licensed the Lotus coating technology from NASA Goddard Space Flight Center (GSFC) for possible integration into our louver design [7]. This lightweight and thin coating offers passive dust mitigation capability. We are maturing this technology separately, and if successful, we will integrate it into our system by applying this coating to the outer surface of our louver vanes exposed to the environment.

During Year 1 of this project, we have designed, constructed and evaluated the performance of one module of the overall device under laboratory conditions [8]. Photographs of the module with the vanes in closed and open positions are shown in Figure 1. In this version, we mounted the motor to the top vane, and the remaining vanes are controlled by the rotation of the top vane. Results from laboratory measurements under earth conditions are discussed in detail in this paper. Also included is a brief summary of our plan to evaluate the louver module under lunar surface conditions that can be simulated in the cryogenic vacuum chamber at NASA JSC.



(a) **(b)**

Figure 1: Photographs of the actively controlled louver module with vanes in closed and open positions.

EVALUATION OF LOUVER FUNCTIONALITY AND PERFORMANCE

We have performed a series of tests to determine the time needed to open and close the vanes as well as the power and energy needed to operate the motor. We then examined the ability of our

Trade names and trademarks are used in this report for identification only. Their usage does not constitute an official endorsement, either expressed or implied, by the National Aeronautics and Space Administration.

louver module in attenuating two types of ionizing radiation expected in the Van Allen belts. We used the Transmotec motor to open and the louver vanes in these tests. We then evaluated the ability of the louver module to reduce the radiative heat loss (for example, to reduce the heat loss from the radiator during the lunar night) and to mitigate the dust transport to the radiator. The test methods and key results from these studies are discussed below.

Functionality Testing

We performed functionality testing with two different louver modules. The first module had dimensions of 31" × 31" and was constructed from 6 individual vanes that were controlled using a non-space rated Transmotec motor, while the second module was smaller (26" × 26"), had 5 vanes and was controlled using an off-the-shelf Maxon motor. We present the tests with the first module equipped with Transmotec motor here.

As a part of functionality testing, we performed several openings and closings of the vanes in the louver module. We oriented the module vertically for these tests as shown in Figure 1. The motor vendor recommends operating it using a DC voltage of 12 V, but the voltage can be lowered to reduce the vane speed as well as energy consumption. We have examined the effect of varying the voltage supplied to the motor on the average time, current, power, and energy needed to open/close the vanes in the module. We performed about 5 openings and closings at each voltage and averaged the time needed to open/close the vanes as well as the current and power consumption. We then calculated the energy consumption for vane operation from the measured power and time values. These results are summarized in Table 1. As the voltage applied to the motor was increased from 4 to 12 VDC, the time needed to open/close the vanes decreased from an average of 1.73 s to 0.58 s. The current needed for motor operation varied between 0.43 A to 0.3 A over the range of applied voltages. The power needed to operate the motor increased from 1.7 W to 5 W, as the applied voltage was increased from 4 to 12 VDC. Finally, the energy consumption varied between 2.9 J and 1.9 J for the different applied voltage levels. We propose to operate the motor using 10 VDC that provides activation in ~0.6 s and consumes <2 J of energy. Assuming that the louver vanes are opened or closed once every 14 days, we need to open/close them 260 times over a 10-year period, and it will consume about 520 J of energy which is insignificant. Despite opening and closing several times, the louver maintained its form and function.

Table 1: Key results from functionality testing of our louver module.

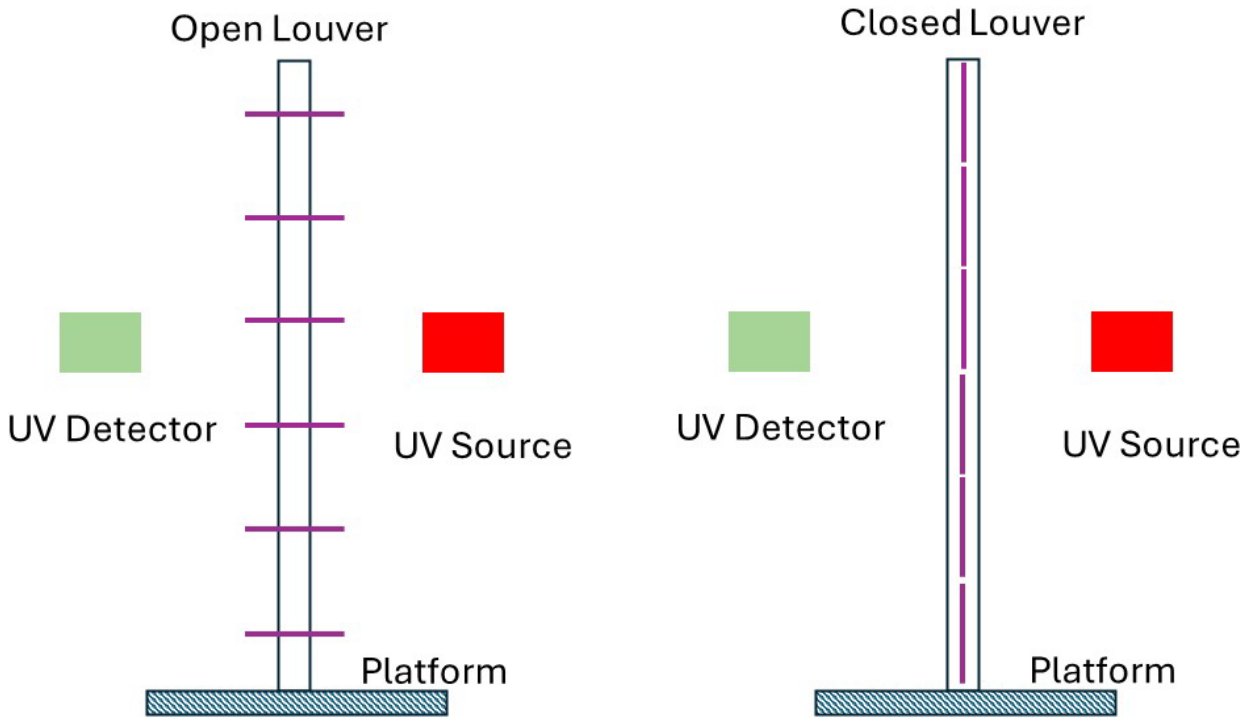
Voltage (V)	Time (s)	Current (A)	Power (W)	Energy (J)
4	1.73	0.43	1.7	2.9
6	1.09	0.40	2.4	2.6
8	0.93	0.34	2.7	2.5
10	0.62	0.30	3.0	1.9
12	0.58	0.42	5.0	2.9

UV Attenuation

A schematic of the test setup used for the UV attenuation tests is shown in Figure 2. It consists of a UV source (TactEagle's UVA-T7) that generates ~360 nm wavelength UV rays with an

Trade names and trademarks are used in this report for identification only. Their usage does not constitute an official endorsement, either expressed or implied, by the National Aeronautics and Space Administration.

estimated energy of 3.5 eV. It was oriented in our tests to send UV rays towards the louver as shown in Figure 2. A UV detector (SolarMeter Model 7.0) was located across from the UV source on the other side of the louver as shown in the figure. In our tests, this UV detector simulates the radiator surface that receives high energy ionizing radiation from outside (simulated with the UV bulb). We controlled the UV power that reaches the sensor by varying the distance between the source and the detector. We performed measurements with the vanes in open position as illustrated in Figure 2 (a) to allow most of the radiation to reach the detector that closely mimics the condition of baseline case of no protection because our vanes are thin and intercept very little radiation. We then performed the same measurements with the louver vanes in closed position as illustrated in Figure 2 (b) to examine the UV attenuation capability of our device.



(a) Louver with open vanes. **(b) Louver with closed vanes.**

Figure 2: Schematic of test setup used to measure the UV radiation attenuation across the louver.

We conducted 12 tests in this series out of which 6 were performed with the louver vanes in open position and 6 with the vanes in closed position. The results from these measurements are summarized in Table 1. In test UVL-1, we positioned the UV source very close to the louver (with a separation distance of less than 0.2 inches) and measured a transmitted UV radiation level of 1.9 mW with the louver vanes in open position. When we closed the vanes in test UVL-2, the transmitted UV radiation level at the detector dropped to 0 mW showing that we obtained 100% attenuation. As we moved the UV source away from the louver with separation distances of 0.5 to 3 inches in subsequent tests, the transmitted UV radiation level across the louver with open vanes

Trade names and trademarks are used in this report for identification only. Their usage does not constitute an official endorsement, either expressed or implied, by the National Aeronautics and Space Administration.

decreased from 1.6 mW to 0.1 mW. Closing the louver vanes decreased the UV transmission to 0 mW in each of these tests.

These data suggest that our louver in closed position can attenuate 100% of the UV radiation. These results are consistent with [8] that suggests that we need less than 0.8 μm thick alloy to attenuate the 3.5 eV UV radiation.

Table 2: Summary of results from UV transmission tests across the louver with the vanes in open and closed positions.

Test	Distance from Louver (inches)	Power (mW)		UV Attenuation
		Open Louver	Closed Louver	%
UVL-1, 2	<0.2	1.9	0	100
UVL-3, 4	0.5	1.6	0	100
UVL-5, 6	1	1.2	0	100
UVL-7, 8	1.5	1	0	100
UVL-9, 10	2	0.5	0	100
UV-11, 12	3	0.1	0	100

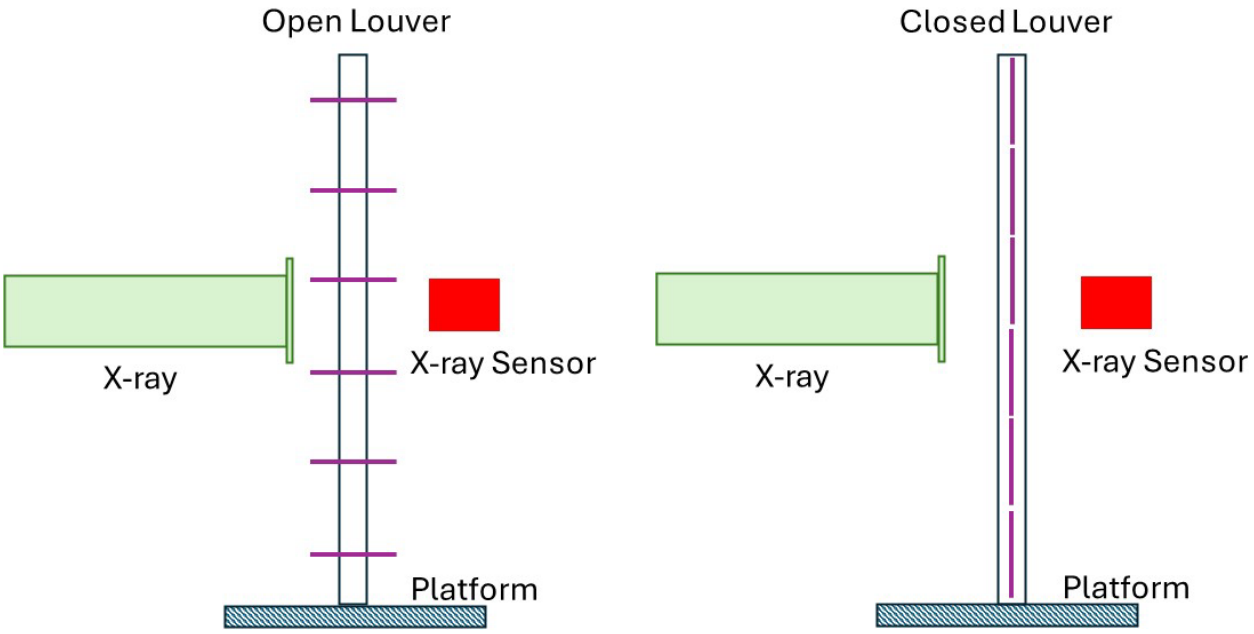
X-Ray Attenuation

We performed a series of tests to examine the X-ray attenuation capability of our louver module. X-rays are a much higher energy radiation form that may be of interest in the Van Allen belts. A schematic of the setup used for these tests is shown in Figure 3. We used an Instrumentarium Model Focus X-ray to illuminate the target region. It uses 60 – 70 kV and 7 mA, and can generate X-ray radiation with pulse widths up to 1 s. We positioned the X-ray source in front of the louver as shown in Figure 3. We used the Reed instruments' Model R8008 sensor to measure the transmitted X-ray radiation through the louver. In our test apparatus, the X-ray tube simulates the high energy radiation from the Van Allen belts, and the Reed Instruments' sensor simulates the radiator surface. We positioned the sensor across from the X-ray source on the other side of the louver as illustrated in Figure 3. We performed 5 sets of measurements. In each set, we performed one test with the louver vanes in open position (as illustrated in Figure 3 (a)) followed by a test with the vanes closed (Figure 3 (b)). The measured X-ray transmissions in test 1 with a 70 keV X-ray are presented in Figure 4 (a). When the vanes were in open position, we obtained an X-ray transmission level of 85.6 μSieverts/hr across the louver, that dopped to 33.8 μSieverts/hr when we closed the vanes. Data from test 6 in which we used a 60 keV X-ray are shown in Figure 4 (b). When the vanes were in open position, we observed a transmission of 71.5 μSieverts/hr that dropped to 22.2 μSieverts/hr when we closed the vanes.

Data from all the tests conducted with 70 keV and 60 keV X-rays are summarized in Table 2. In each test, we found that the X-ray transmission decreased significantly when we closed the louver vanes. We averaged the results from all the tests conducted with 70 keV X-rays and obtained a mean extinction of 57% across the louver that is caused by the closing of the vanes. Application of Beer's law yields a mean X-ray attenuation coefficient of 42 cm^{-1} from these tests [8]. Similarly, we obtained a higher average extinction of 69% across the closed louver with 60 keV X-rays that corresponds to a mean extinction coefficient of 58.5 cm^{-1}. For comparison, the theoretical optical extinction coefficient of aluminum (the material of construction of SOA passive louvers) is ~0.75

Trade names and trademarks are used in this report for identification only. Their usage does not constitute an official endorsement, either expressed or implied, by the National Aeronautics and Space Administration.

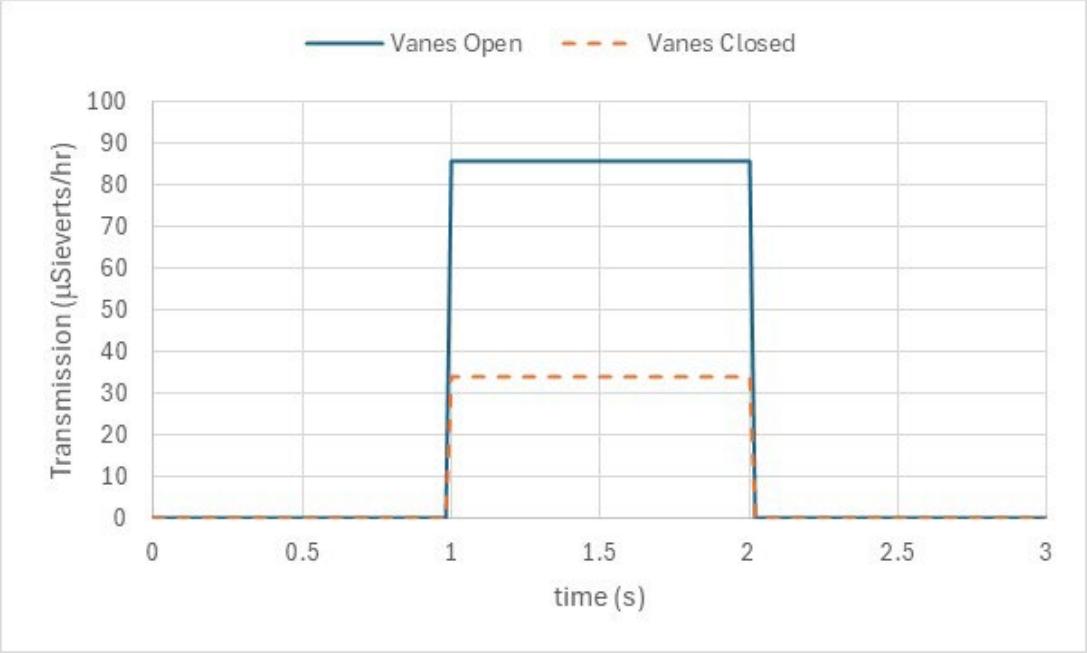
cm^{-1} for at 60 keV X-rays and 0.65 cm^{-1} for 70 keV [9]. Therefore, the optical extinction coefficients with our louvers is 65 – 78× that for current passive louvers for X-rays. This clearly shows that our louver with custom alloy offers much higher radiation attenuation than aluminum-based SOA louvers. This allows us to use much thinner vanes which in turn reduces the device mass as well as the load on the motor used for actuation.



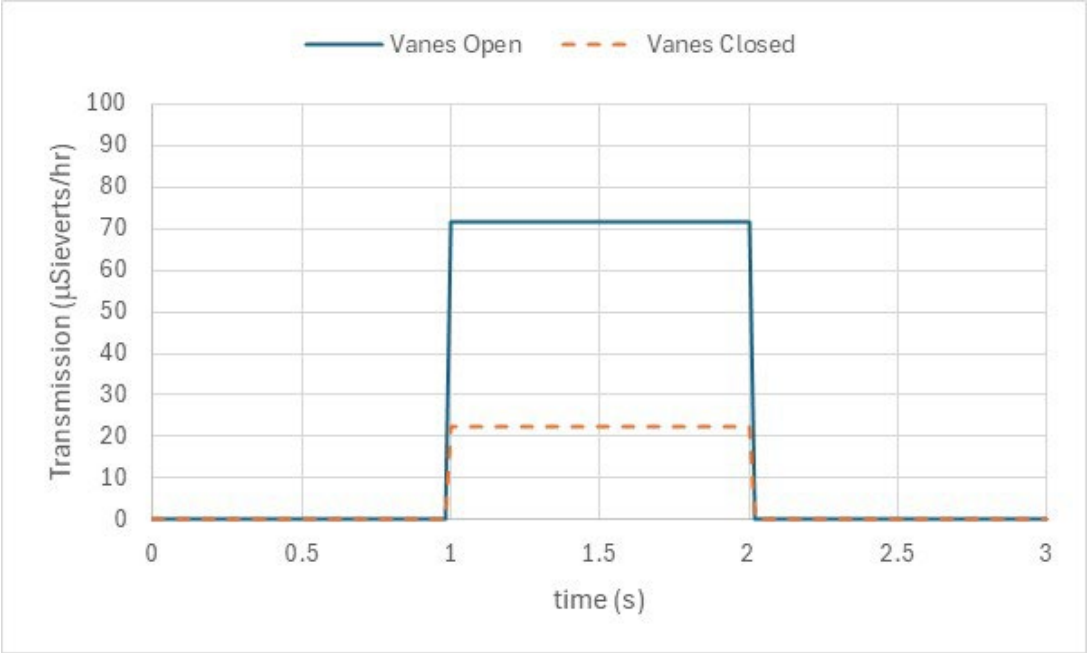
(a) Louver with open vanes. **(b) Louver with closed vanes.**

Figure 3: Schematic of test setup used to measure the X-ray transmission across the louver.

Trade names and trademarks are used in this report for identification only. Their usage does not constitute an official endorsement, either expressed or implied, by the National Aeronautics and Space Administration.



(a) Data from Test 1 with 70 keV X-ray.



(b) Data from Test 6 with 60 keV X-ray.

Figure 4: Sample data from two sets of X-ray attenuation tests with open and closed louvers.

Trade names and trademarks are used in this report for identification only. Their usage does not constitute an official endorsement, either expressed or implied, by the National Aeronautics and Space Administration.

Table 3: Summary of Results from X-ray Attenuation Tests Across the Louver with the Vanes in Open and Closed Positions.

Test	Transmission (μSieverts/hr)	
	vanes open	**vanes closed**
70 keV X-ray		
1	85.63	33.82
2	75.93	33.82
3	76.67	31.77
4	76.67	31.77
5	77.45	38.65
Average	**78.47**	**33.97**
60 keV X-ray		
6	71.5	22.24
7	69.3	27.68
8	70.03	17.27
9	78.15	17.27
10	72.24	27.68
Average	**72.24**	**22.43**

Heat Loss Mitigation Tests

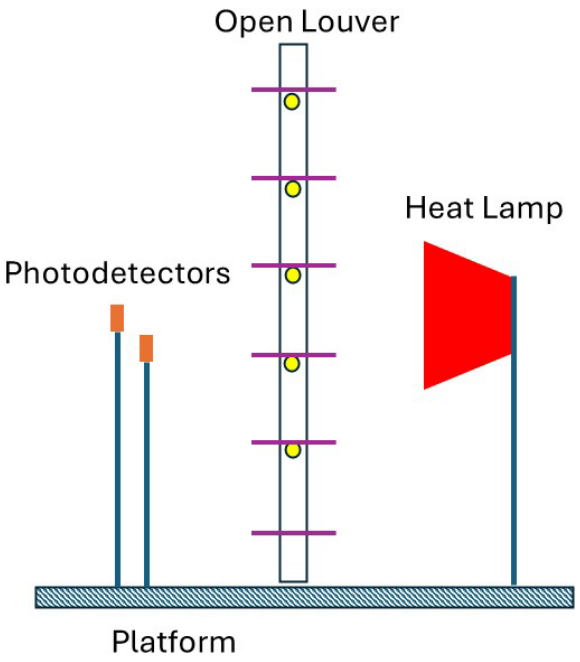
The ambient temperatures on the surface of the moon may drop below -200°C during the cold lunar night near the poles. Exposure to such temperatures can cause the radiator to lose heat excessively which in turn can freeze the coolants compromising its integrity. Our louver with the vanes in closed position can protect the radiator by reducing the heat loss. However, evaluating the effectiveness of our louver in mitigating excessive heat loss under these conditions requires exposure to vacuum and cryogenic conditions which are planned in the coming months (at the JSC cryogenic vacuum chamber). In the meantime, we performed heat loss measurements under atmospheric pressure and room temperature (laboratory conditions) using the test apparatus shown in Figure 5. We used an incandescent light bulb as the heat source to simulate the radiator. This light bulb was positioned near the mid-axis of the louver as shown in the figure. We adjusted the distance between the light fixture and the louver such that most of the radiation from the light bulb is incident on the louver (with little that dispersed elsewhere). The filament in the incandescent light bulb reaches ~2700 K which yield thermal radiation spanning a broad range of wavelengths centered around 1.07 μm including a fraction of the radiation within the visible wavelength range of 0.4 – 0.8 μm. When this thermal radiation is incident on the louver, most of it is reflected towards the light bulb, some of it is absorbed and the rest is transmitted through the small gaps between the louver vanes (radiation loss). Absorption of thermal radiation causes the louver vanes to heat up over time, and we captured it by measuring the louver temperature. We captured the transmission across the louver by measuring the visible portion of the transmitted radiation. We installed two Newport photo diode sensors (P1 and P2) in front of the louver assembly (across from the light bulb) that are offset from each other by about two inches. We installed seven K-type thermocouples at different locations on the louver vanes to track the local temperature versus time

Trade names and trademarks are used in this report for identification only. Their usage does not constitute an official endorsement, either expressed or implied, by the National Aeronautics and Space Administration.

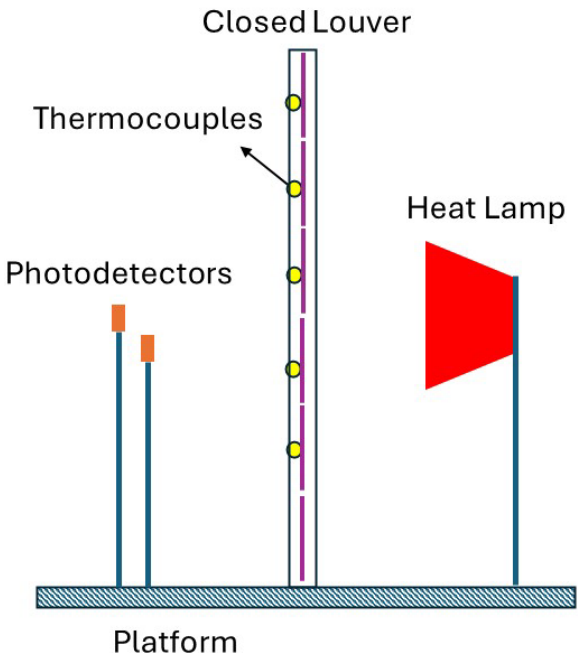
induced by the absorption by the vane from the fraction of light bulb's thermal radiation. The thermocouple placement is shown in Figure 6. We installed 3 thermocouples on the fourth vane from the top, and one thermocouple on each of the other vanes except the bottom vane (i.e., on vane 6). The outputs from the seven thermocouples were collected using the Graphtech Midi Logger Model GL240. Since changes happen relatively slowly, we set a data collection rate of 1 sample/s from the thermocouples for these tests. The outputs from the photosensors were read off the digital output at 1 sample/min. Note that the heat lamp simulates the radiator surface and the photometers simulate the lunar environment in this test.

We performed five tests with the vanes oriented in three positions:

1. **Completely open**, in which the vanes were normal to the plane of the louver and approximately parallel to the light rays from the bulb as illustrated in Figure 5 (a). Since the louver vanes were thin, they intercepted a very small fraction of the incoming radiation and let most of the thermal radiation to transmit across.
2. **Completely closed**, in which the vanes were parallel to the plane of the louver as illustrated in Figure 5 (b) to block most of the thermal radiation. In this configuration, a very small fraction of the radiation can leak through the gaps between the individual vanes.
3. **Partially open**, in which the vanes were oriented at an angle of 45° with respect to the plane of the louver, in which the louver blocked a significant fraction of the thermal radiation.

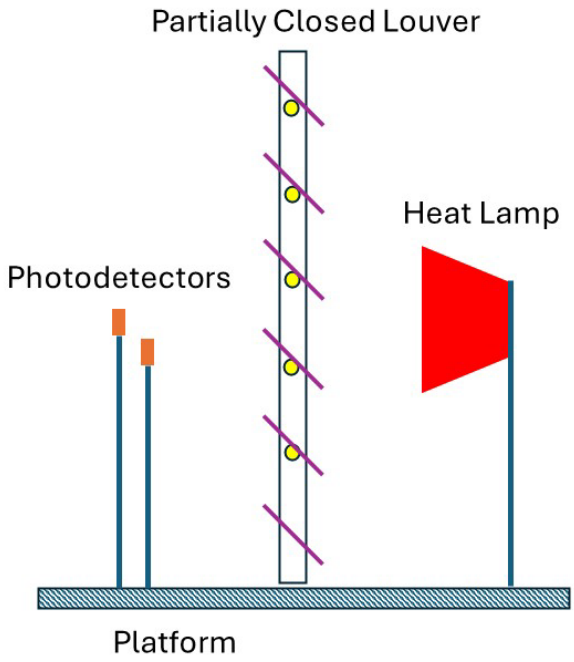


(a) Louver with open vanes.



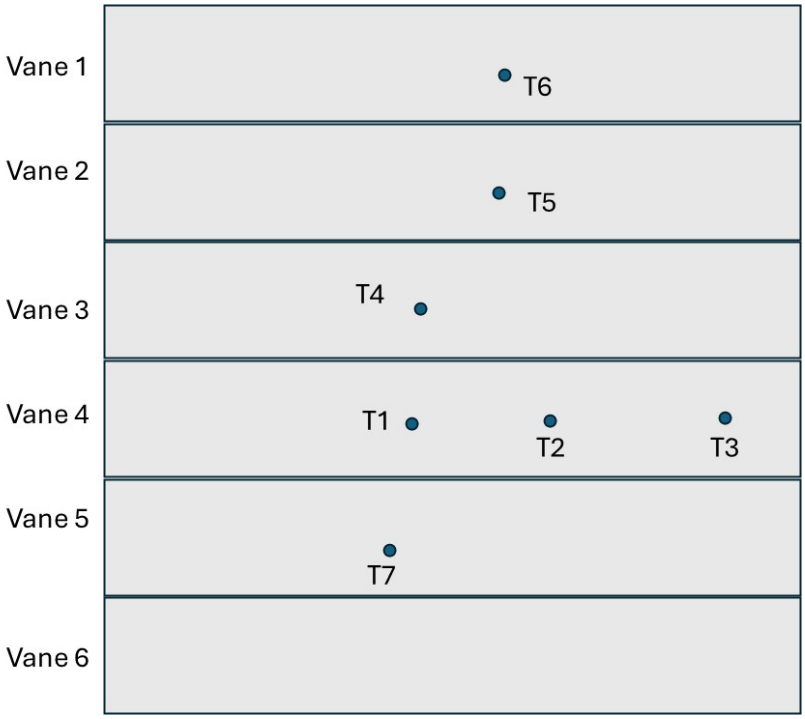
(b) Louver with closed vanes.

Trade names and trademarks are used in this report for identification only. Their usage does not constitute an official endorsement, either expressed or implied, by the National Aeronautics and Space Administration.



(c) Louver with partially closed vanes (at 45°).

Figure 5: Schematic of test setup used for thermal radiation transmission measurements.

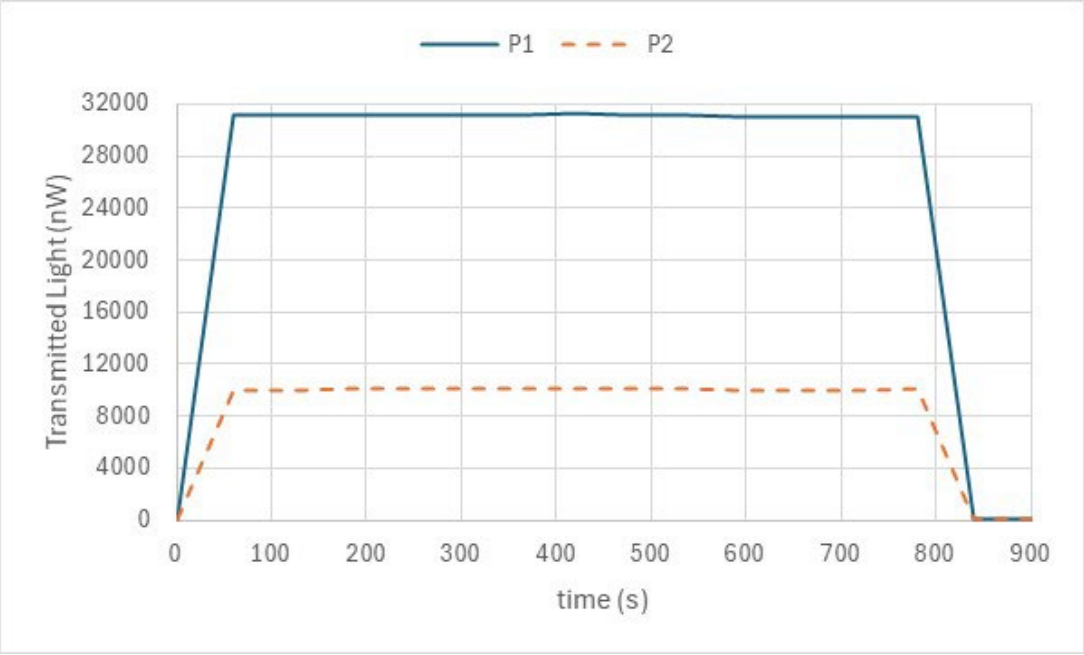


Trade names and trademarks are used in this report for identification only. Their usage does not constitute an official endorsement, either expressed or implied, by the National Aeronautics and Space Administration.

Figure 6: Thermocouple placement used in our tests to measure the extent of thermal radiation absorption by louver vanes.

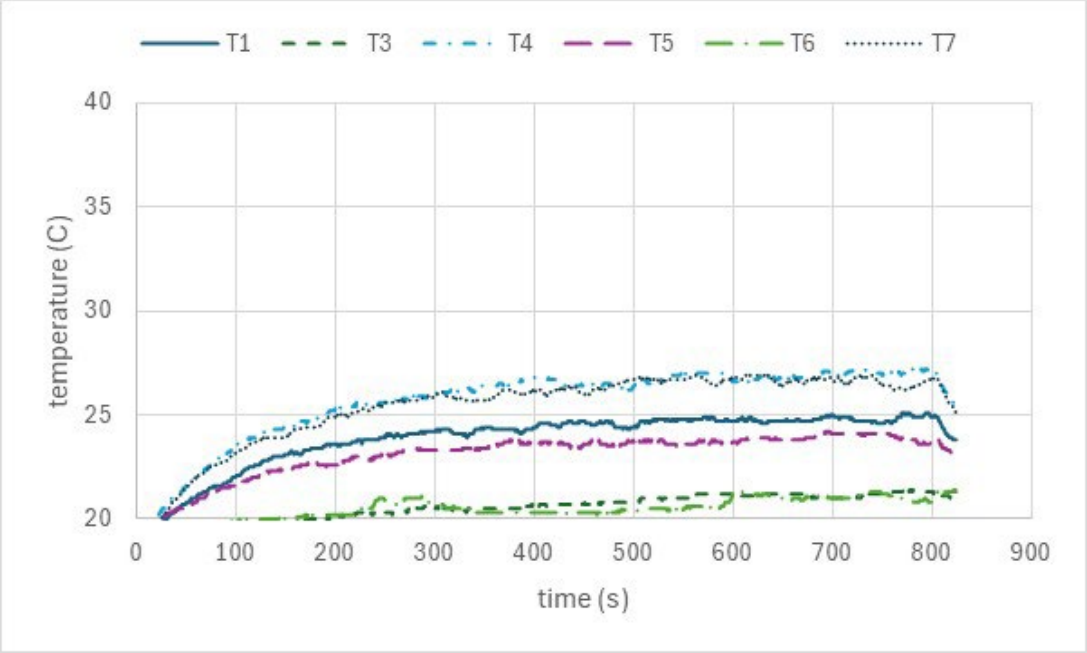
We performed test RAD1 with the vanes in open position to allow most of the thermal radiation from the heat lamp to pass through the louver. The visible fraction of this radiation was captured using the two photo diode sensors, P1 and P2. We opened the louver vanes, turned the lightbulb on, and started the data collection. Even though the radiation level peaked right away, our slow data collection with the photo sensors P1 and P2 led to the gradual rise between 0 and 60 s. Due to variations in positions and calibrations, the two photosensors captured different radiation levels. The visible fraction of the thermal radiation from the heat lamp reaching the detector P1 reached a peak of 31,131 nW where it remained until we turned the heat lamp off about 780 s into the test. The radiation at detector P2, on the other hand, reached a peak of only 10,058 nW where it remained until the heat lamp was turned off. Note that even when the vanes were in open position, a small fraction of the incoming radiation that reaches the louver is intercepted by the thickness of the vanes and the aluminum structure that supports the vanes. The resulting absorption of thermal radiation by the louver raised its temperature slightly as shown in Figure 7. Out of our 7 thermocouples, one (Thermocouple #2 in Figure 6) malfunctioned during the tests, and we excluded it from the figure. The temperature of vanes 4 and 7 exhibited the largest increases in temperature with a maximum ΔT of 7°C, while vane 1 and the thermocouple close to the edge of vane 4 exhibited the lowest maximum ΔTs of 1.3°C. The latter is because these two thermocouples are near the edges of the radiation cone created by the thermal lamp.

Closing the vanes in test RAD2 caused the louver to intercept most of the thermal radiation which reduced the transmission drastically to 258 nW at P1 and 43 nW at P2 as shown in Figure 8. Thermal absorption by the louver vanes increased in RAD2 leading to maximum ΔT of 17.4°C at the middle of vane 4 (that is located directly in front of the thermal lamp). We observed the lowest ΔT of 3.9°C near the edge of vane 4.



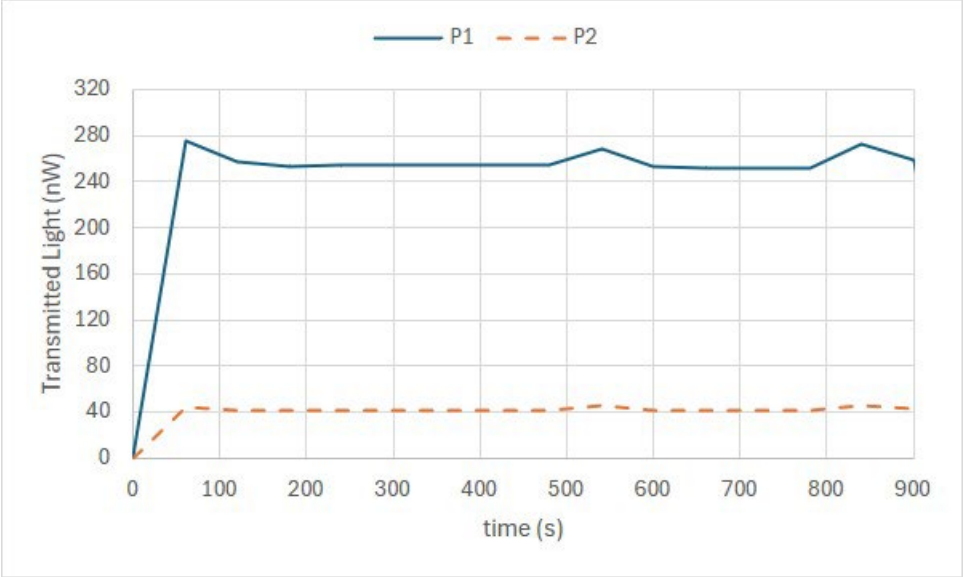
Trade names and trademarks are used in this report for identification only. Their usage does not constitute an official endorsement, either expressed or implied, by the National Aeronautics and Space Administration.

(a) Thermal radiative transmission across the louver versus time.



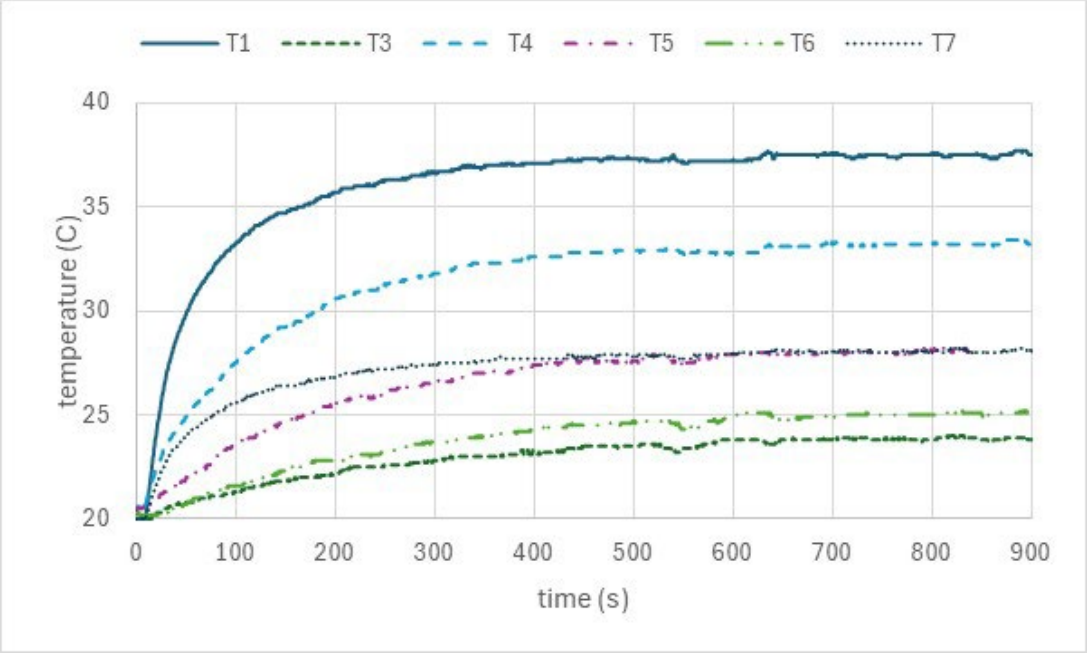
(b) Thermal radiation absorption measured using thermocouples mounted on vanes.

Figure 7: Data from thermal radiative heat loss measurements from test RAD1 across the louver with open vanes.



(a) Radiative transmission measurements.

Trade names and trademarks are used in this report for identification only. Their usage does not constitute an official endorsement, either expressed or implied, by the National Aeronautics and Space Administration.

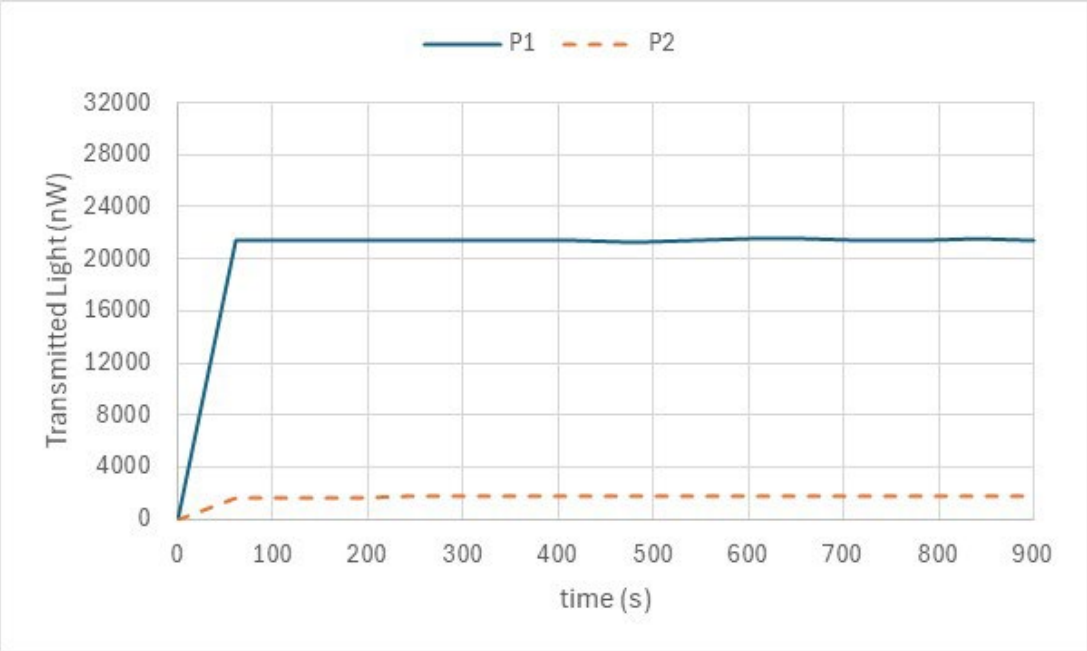


(b) Thermal radiation absorption measured using thermocouples mounted on vanes.

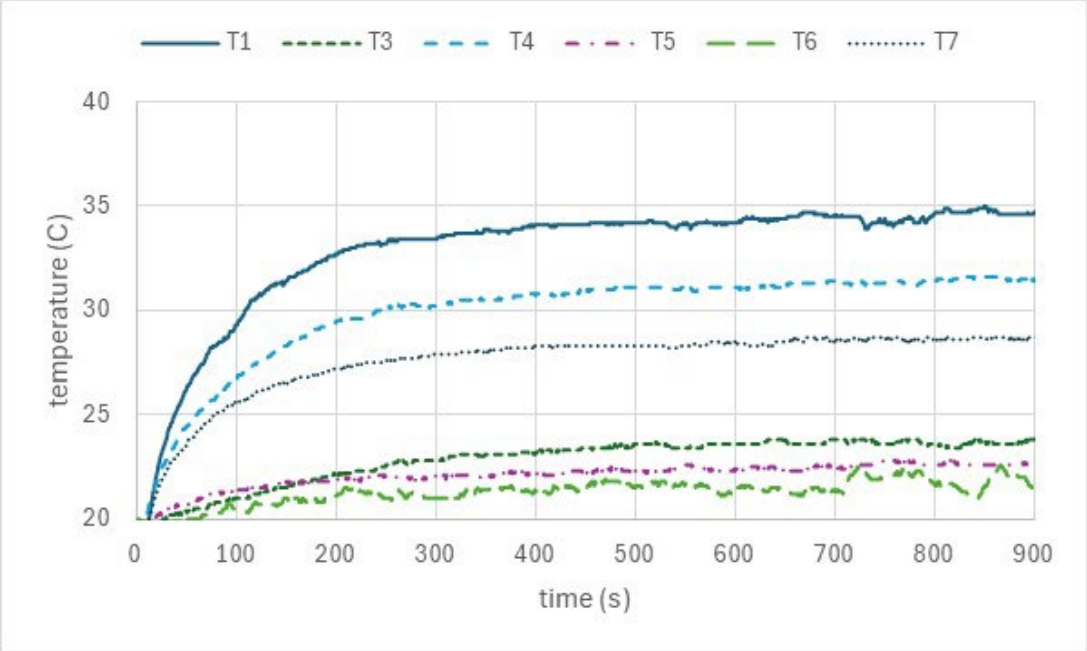
Figure 8: Data from thermal radiative heat loss measurements from test RAD2 across the louver with closed vanes.

Data from test RAD5 in which we closed the vanes partially are shown in Figure 9. Angling the vanes caused some of the radiation to be intercepted by the louver vanes and allowed more radiation to be transmitted relative to the closed vane scenario. We observed peak transmissions of 21,400 nW at P1 and 1,693 nW at P2 in this test, and maximum ΔTs between 2.9°C at vane 1 (near the edge of radiation cone from the light bulb) and 14.9°C at the middle of Vane 4 (near the middle of the radiation cone).

Trade names and trademarks are used in this report for identification only. Their usage does not constitute an official endorsement, either expressed or implied, by the National Aeronautics and Space Administration.



(a) Radiative transmission measurements.



(b) Thermal radiation absorption measured using thermocouples mounted on vanes.

Figure 9: Data from thermal radiative heat loss measurements from test RAD-05 across the louver with partially closed vanes (at 45° with respect to the louver frame).

Key results from the thermal radiation measurements across the louver with the vanes in open, closed, and partially open positions are summarized in Table 3. Tests RAD1 and RAD4 with the

Trade names and trademarks are used in this report for identification only. Their usage does not constitute an official endorsement, either expressed or implied, by the National Aeronautics and Space Administration.

vanes in open position yielded peak thermal radiation levels of 30,053 to 31,131 nW at P1 and 9899 to 10,058 nW at P2. Closing the vanes dropped the transmitted radiation to 117 to 258 nW at P1 and 42 to 43 nW at P2. (We noted that the vanes did not close completely in RAD2 leaving a small gap between the vane edges that might have contributed to the slightly higher transmission at P1. Closing it more tightly dropped the transmission in RAD3.) Orienting the vanes at 45° to obtain partial closure yielded thermal transmission values between the completely open and completely closed cases, as expected. Even though a small fraction of the incoming radiation was intercepted by the vane edges and the vane support structure, we neglected these effects and assumed 100% transmission in tests RAD1 and RAD4. Closing the vanes reduced the transmission (i.e., radiative leakage) by more than 99.5% in test RAD3. Closing the vanes partially led to differences in transmission depending on the relative positions of the photodetectors with respect to the light source and vane edges. Absorption of some of the thermal radiation incident on the louver vanes raised their temperatures as measured by the thermocouples mounted on the vanes. The average rises in temperatures across all the thermocouples in each of the tests are presented in Table 3. Using the thermocouple data from each vane, we calculated the thermal energy absorbed by the louver in each test. With the vanes in open position, the louver absorbed about 1,755 J of energy, while closing the louvers increased it to 2,826 to 3,249 J. Partially closing the louvers caused 2,379 J of energy absorption. Assuming that 50% of the energy supplied to the heat lamp over the duration of each test was incident on the louver (if the rest was lost due to conversion efficiencies, radiation spread outside the louver surface, heat losses from the bulb to air, etc.), we calculated the percent of radiation absorbed by the louver shown in the last column of the table.

The above data showed that closing the vanes led to a very small fraction of the radiation being transmitted across the louver (~0.43%) and a slightly larger fraction (~2.41%) being absorbed by the louver vanes, while the remaining >97% is reflected. Partial closure of the vanes caused transmission that varied significantly depending on the detector position relative to the vanes and radiation absorption that was between the open and closed vane scenarios. These results suggest that (i) complete closure of vanes minimizes heat loss from the radiator during the lunar night near the poles, and (ii) partial vane closure can be an option to help the radiator reject heat while protecting it from dust and sunlight (depending on solar elevation and the radiator/louver orientation).

Table 4: Summary of Key Results from the Thermal Radiative Heat Loss Measurements Across the Louver with Open, Closed and Partially Closed Vanes.

Vane Orientation	Test	Thermal Radiation Transmission				Thermal Radiation Absorption		
		P1 (nW)	P2 (nW)	% Transmission		ΔT_{ave} (°C)	Absorption (J)	Absorption (%)
Open	RAD1	31131	10058	100	100	4.3	1758	1.3
Closed	RAD2*	258	42	0.83	0.42	8.10	2826	2.09
Closed	RAD3	117	43	0.39	0.43	9.10	3249	2.41
Open	RAD4	30053	9899	100	100	4.20	1753	1.3
Open at 45°	RAD5	21402	1693	71.2	17.1	6.40	2379	1.76

* Vanes did not close completely leaving a small gap between the vanes that caused some radiative leakage

Trade names and trademarks are used in this report for identification only. Their usage does not constitute an official endorsement, either expressed or implied, by the National Aeronautics and Space Administration.

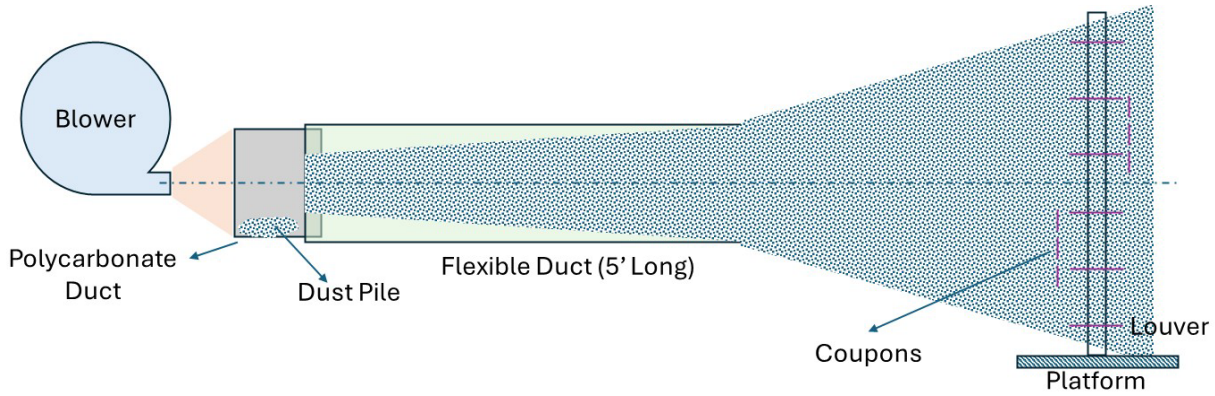
Dust Mitigation Tests

Landing on the moon and surface operations are likely to propel the highly charged dust particles that travel in all directions. Due to a lack of an atmosphere, the dust particles travel ballistically towards the radiator. Installing a louver with the vanes in closed position is likely to intercept most of these particles keeping the radiator surface clean. As an aside, we are maturing the Lotus coating to prevent these particles from collecting on the louver vanes. Until this development is completed, we decided to use the uncoated louver for dust mitigation. We have developed a test apparatus to evaluate the effectiveness of vanes in reducing the dust transport across the louver module. We understand that the primary mode of dust transport is carriage by air molecules in this setup that is quite different from the ballistic transport on the moon. We still decided to perform preliminary tests where dust particles were entrained in air, while we await the vacuum chamber tests at JSC later in this project where ballistic dust transport will be examined.

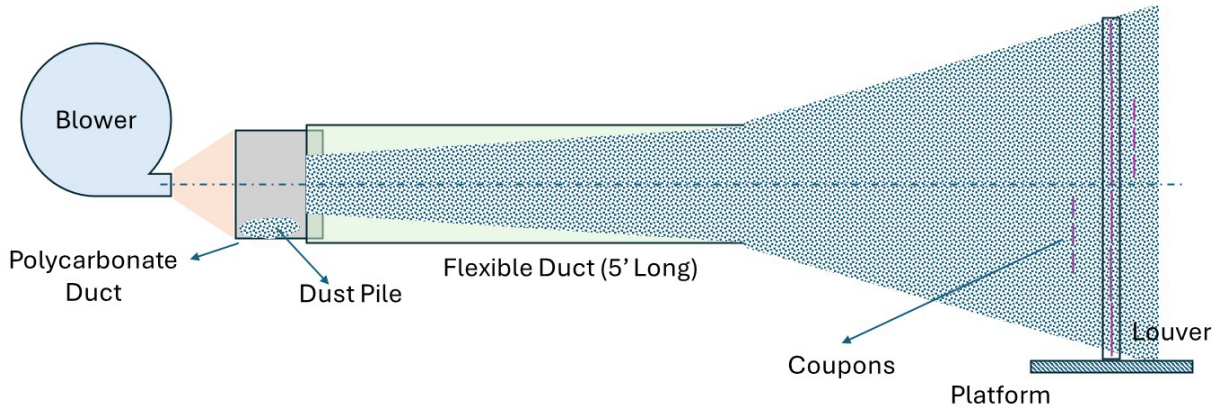
A schematic of this test setup is shown in Figure 10. It uses a 210 CFM air blower to generate the dust laden air flow directed towards our device. This air flow from the blower enters a 2-foot-long polycarbonate duct with an inner diameter of about 8 inches where the gas expands radially and fills a portion of the radial cross section of the duct. We created a pile of fine particulate talc (used as a morphological simulant of lunar dust) on the floor of the polycarbonate duct approximately 18 inches from the blower exit. After exiting the polycarbonate duct, the carrier air along with the entrained dust particles then enters a flexible duct with an inside diameter of ~9.25” and a length of 5 feet. After exiting the flexible duct, the aerosol plume entrains clean ambient air, expands and undergoes dilution as it flows towards the target region. We placed the louver mounted on a platform a few feet away from the duct exit to ensure that it intercepts the aerosol plume as shown in Figure 10. The air speed decreases from 2.2 m/s at the exit of the flexible duct to 0.22 m/s near the louver. The slow speed is desirable to simulate atmospheric aerosol. We used optically transparent microscope slides with dimensions of 76 mm (height), 25 mm (width) and 1 mm (thickness) to simulate the radiator surface. We placed three vertically oriented coupons in front of the louver to intercept a portion of the aerosol plume as shown in Figure 10 and simulate an unprotected radiator surface. We placed three identical coupons behind the louver. We simultaneously measured the dust adhesion on the coupons in front of and behind the louver with the louver vanes in open and closed position in each test to ensure that both sets of coupons are exposed to the same aerosol concentration and flow rate.

We performed the first test with the louver vanes in open position as illustrated in Figure 10 (a). All the 6 coupons were oriented to face the aerosol outlet from the apparatus as shown in the figure. Once we turned the blower on to start the test, it took about 1 minute for the entire dust pile to be aerosolized. We then stopped the test and extracted one unprotected coupon (#1) from the front of the louver and one coupon (#4) from behind the louver that have been exposed to dust for 1 minute. Since most of the dust was depleted after 1 minute, we added another ~20 g of dust to the polycarbonate duct and aerosolized it for another 1 minute after which we extracted one unprotected coupon (#2) from the front of the louver and another coupon (#5) from behind the louver. These coupons were exposed to dust for a total of 2 minutes. We then continued with the addition of another 20 g of dust and aerosolization for 1 minute. After this, we extracted the last set of coupons (#3 from the front of the louver and #6 from the back of the louver) that were exposed to 3 minutes of dust aerosol.

Trade names and trademarks are used in this report for identification only. Their usage does not constitute an official endorsement, either expressed or implied, by the National Aeronautics and Space Administration.



(a) Louver with open vanes.



(b) Louver with closed vanes.

Figure 10: Schematic of the test apparatus used to evaluate the effectiveness of ASP's louvers in mitigating dust adhesion to target surfaces.

We performed laser transmission measurements across the coupons extracted from the test apparatus above. This was done by illuminating a portion of the coupon with a collimated HeNe laser beam and measuring the laser power that is transmitted across the dust layer and the optically transparent substrate. The transmission loss (or optical extinction) correlates to the mass of dust aerosol in the illuminated region. Since the dust may not coat the coupon uniformly, we performed measurements at 5 different locations on each glass slide and used the average values to represent each test condition. Clean quartz glass coupons transmitted almost the entire radiation (~8 mW) that corresponds to a 0 minute exposure to dust cloud. Unprotected coupon in front of the louver exposed to one minute of dust aerosol yielded a transmission of 7.88 mW, while the coupon behind the louver with open vanes yielded 7.63 mW. After 2 minutes of dust exposure, the transmitted light power decreased to 7.75 mW in front of the louver and 7.14 behind the louver. Finally, after 3 minutes of dust exposure, the transmitted light power decreased further to 7 mW in front of the louver and 6.92 mW behind the louver. The differences between the observed transmitted laser power in front of the louver and behind it could be due to variations in local dust concentration and partial protection provided by the vane thickness and the support structure.

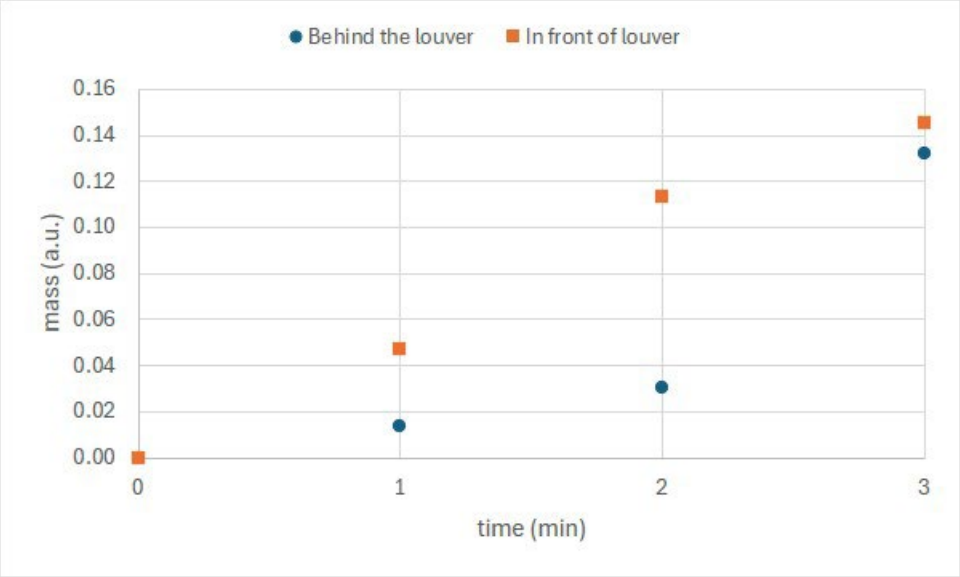
Trade names and trademarks are used in this report for identification only. Their usage does not constitute an official endorsement, either expressed or implied, by the National Aeronautics and Space Administration.

We performed a second test in which the louver vanes were in closed position. Except for the vane closure, the test procedure was identical to the above. We extracted three coupons in front of the closed louver (#7, 8 and 9) and three coupons from behind the closed louver (#10, 11, and 12) after 1, 2 and 3 minutes of exposure to dust aerosol. The transmitted laser power changed very little over time behind the louver varying between 8.3 mW and 8.23 mW. This slight drop is due to a small amount of dust that reached the coupons possibly through the small gaps between the louver vanes. The transmitted laser power decreased significantly from 8.3 mW to 7.77 mW after 1 minute, 7.34 mW after 2 minutes and 7.24 mW after 3 minutes for the unprotected coupons in front of the louver.

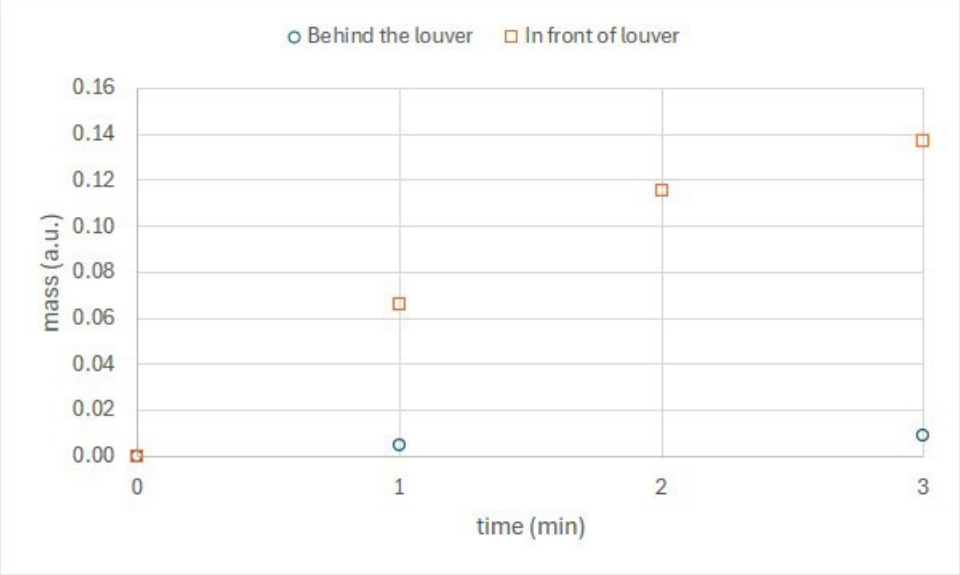
We calculated the mass of aerosol collecting in the laser illuminated detection regions from coupons extracted from different tests above. The mass of dust collecting on the coupons (expressed in arbitrary units or a.u.) in front of and behind the louver in the test with open vanes are plotted in Figure 11 (a). During 3 minutes of exposure to the aerosol plume, the mass of dust collecting on the coupon increased to 0.132 units in front of the louver, while it increased to 0.145 units behind the louver with open vanes. This small difference could be due to spatial variations in the dust concentrations at the two locations, and partial protection provided by the vane thickness and the vane support frame. In the test with the vanes in closed position, the mass of dust increased to 0.137 units in the unprotected coupons in front of the louver, while it increased to only 0.009 units in the protected coupons behind the closed louver as shown in Figure 11 (b). This suggests that closing the louver vanes decreases the mass of dust penetrating the louver (to reach the radiator surface in the final application) by 93.6%.

We expect that the dust mitigation performance of our louver will be much better on the moon because the gas flow used in the above tests might have helped carry some dust through the small gaps between the vanes to reach the coupons behind the louver. This is because the finer fractions of dust aerosol used in our test follow the gas streamlines. As the gas molecules bend around the corners through the gaps between the vanes, the dust particles travel towards the coupons following the gas streamlines. However, dust particles on the lunar surface travel ballistically since there is no atmosphere, which prevents them from bending around the corners of louver vanes to penetrate the device and are more likely to bounce off the vane surfaces (or to bond with and stick to the vanes). Therefore, closing the vanes of our louver is likely to intercept such particles preventing them from reaching the radiator. This should improve the dust mitigation capability of our louver even further in the target application. This will be examined further in the cryogenic vacuum chamber tests planned over the coming months of this project.

Trade names and trademarks are used in this report for identification only. Their usage does not constitute an official endorsement, either expressed or implied, by the National Aeronautics and Space Administration.



(a) Data from test with louver vanes in open position.



(b) Data from test with louver vanes in closed position.

Figure 11: Mass of aerosol collected on the coupons versus time from the two sets of tests with open and closed louver vanes.

PLAN TO EVALUATE LOUVER MODULE UNDER LUNAR SURFACE CONDITIONS

The tests presented in the previous section focused on the evaluation of our louver module under laboratory conditions that represent the temperatures and pressures expected on earth. These data provide some insight into the effectiveness of our louver in protecting the radiator. The next step is to evaluate the louver under lunar surface pressures and temperatures to improve the technology

Trade names and trademarks are used in this report for identification only. Their usage does not constitute an official endorsement, either expressed or implied, by the National Aeronautics and Space Administration.

readiness level. We are currently completing the testing agreement with NASA to perform these tests at the JSC cryogenic vacuum chamber that has internal dimensions of 32" × 32" × 32" and can maintain pressures as low as 10^{-5} to 10^{-7} torr. The temperatures of the 4 side walls as well as the top and the bottom of the chamber can be controlled independently to maintain the chamber interior between -300°F (-185°C) to +300°F (+148°C) during the tests. The vacuum chamber has electrical feedthroughs that can be used to provide power to the motor. Thermocouples can be used to monitor the temperatures of various regions of the chamber during the tests, and their leads can be pulled through the electrical feedthrough. Additional thermocouples can be used to track the temperatures of various regions of the louver and the motor. Glassport on the side of the chamber can be used for optical measurements using instruments located outside the chamber.

We propose to perform 4 types of tests at the JSC cryogenic vacuum chamber facility.

1. **Module functionality under lunar surface pressures and temperatures:** We built most of the components of our louver from materials that have been space tested in the past and are stable at the low temperatures of interest. We are using a motor that is space certified and has been tested to ensure that it remains functional even if it is stored at -150 C. We will evaluate the low temperature and pressure compatibility of the integrated system here.
2. **Outgassing:** The focus is to examine outgassing from the components/materials used in our device when the pressure is reduced to the vacuum levels expected on the lunar surface.
3. **Excessive heat loss mitigation under vacuum and cryogenic conditions:** The objective of these tests is to evaluate heat loss from a radiator exposed to a cold environment across the louver. This is particularly interesting to understand the potential for coolant freezeout when the spacecraft radiator is exposed to the extremely cold lunar environment during nighttime near the poles. In these tests, we propose to simulate the radiator using a hot plate that is heated to ~300 K as illustrated in the left inset of Figure 12. We propose to add insulation to thermally isolate the hot plate and the louver from the chamber walls. The louver will be installed vertically between the hot surface and the optical port as shown in the left inset of Figure 12. The louver will be positioned close to the hot plate to reduce the heat transfer between the hot plate and chamber walls. We propose to monitor: (i) the absorption of thermal radiation from the hot plate by tracking the louver temperatures using thermocouples mounted on the vanes, (ii) transmission and re-radiation of hot surface's thermal radiation across the louver measured using an IR detector located outside the optical window of the chamber, and (iii) power needed to maintain the hot plate at a constant temperature.
4. **Dust mitigation under vacuum conditions:** We propose to orient the louver frame horizontally for these tests as illustrated in Figure 13. The aerosolizer like a vibrating sieve loaded with lunar dust simulant. The aerosolizer will be located above the louver near the top of the chamber. Vibrating the sieve causes the dust particles to rain down vertically under gravity. In this configuration, the radiator is ideally located horizontally near the bottom of the vacuum chamber. We propose to use aluminum coupons coated with Z-93 to simulate the radiator surface in these tests. The louver intercepts some or most of the dust (depending on the vane opening). Dust particles that penetrate the louver will collect on the coupons located at the bottom. We will supplement the coupon dust collection

Trade names and trademarks are used in this report for identification only. Their usage does not constitute an official endorsement, either expressed or implied, by the National Aeronautics and Space Administration.

measurements with direct optical measurements of dust aerosol directly under the louver using a laser and photodetector located outside the vacuum chamber as shown in the right inset of Figure 13. We propose to measure the dust concentrations (both on the coupons and in the environment) with the louver vanes in open and closed positions and use these data to calculate the dust mitigation efficiency of our louver in vacuum conditions.

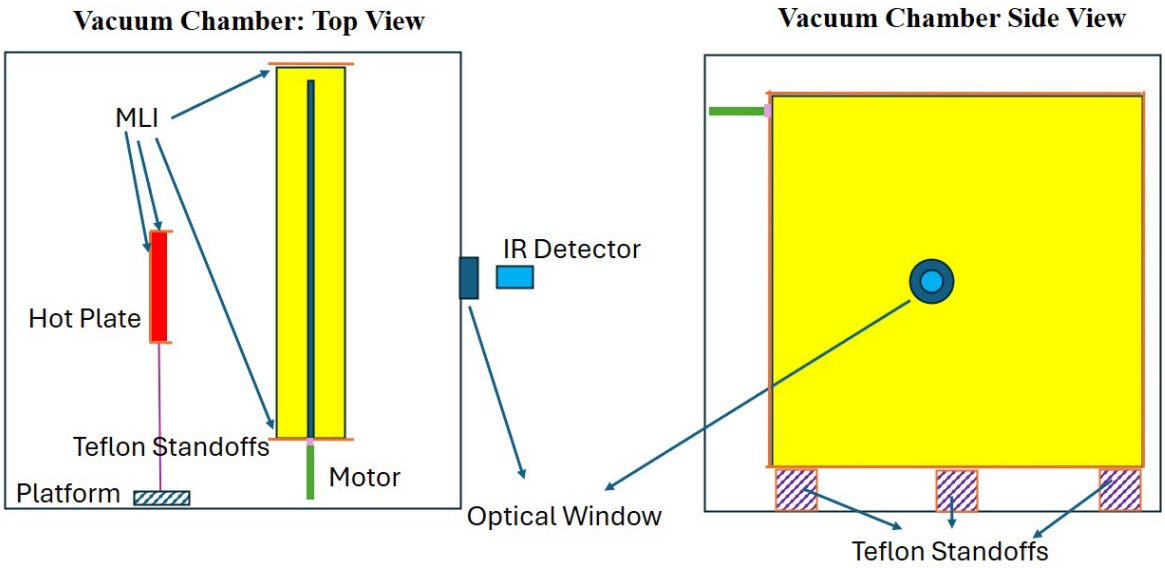


Figure 12: Schematic of the test setup to measure excessive heat loss from the radiator with the louver vanes in open and closed positions.

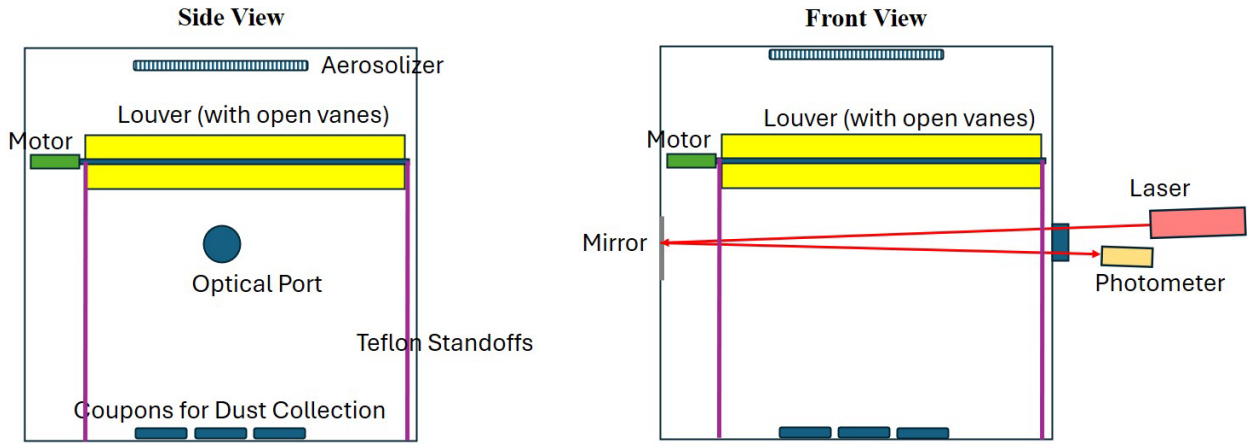


Figure 13: Schematic of test setup to be used for dust mitigation tests.

We are currently completing some customizations to fit our module in the vacuum chamber and survive the chamber conditions. Examples of customizations include reducing the number of vanes in the louver module from 6 to 5, reducing the vane width from 30” to 25”, replacing the off-the-shelf non-space rated motor with space rated motor that can withstand the low temperatures and pressures expected on the lunar surface. Once these steps are completed, we plan to start the cryogenic vacuum testing of our louver module.

Trade names and trademarks are used in this report for identification only. Their usage does not constitute an official endorsement, either expressed or implied, by the National Aeronautics and Space Administration.

CONCLUSIONS AND POTENTIAL APPLICATIONS

The following conclusions can be drawn from the research presented in this paper.

- The spacecraft radiator performance is likely to degrade due to exposure to ionizing radiation during transit through the Van Allen belts, dust during lunar landing and surface operations, and cold environmental conditions during the long lunar night near the poles.
- The state of the art passive louvers are too heavy, too slow, do not offer adequate protection against the above hazards, and are difficult to scale to the larger spacecraft systems needed for future manned missions to the moon and other planetary bodies.
- ASP's actively controlled louvers provide mass savings of ~50% and three orders of magnitude faster activation than SOA passive louvers. Moreover, it requires power intermittently (only to open and close the vanes) and consumes 0.125% of power on an intermittent basis compared to the continuous power loss from unprotected radiators.
- Tests conducted to evaluate the effectiveness of our louver module under terrestrial temperatures and pressures have shown that closing the vanes in ASP's louver can (i) attenuate 100% of 4.5 eV UV rays, (ii) attenuate 57% to 69% of 60 – 70 keV X-rays, (iii) reduce heat loss from the radiator by more than 97% when exposed to cold environmental conditions, and (iv) reduce dust transport to the radiator by more than 93%.
- We propose to conduct additional measurements inside the cryogenic vacuum chamber at NASA JSC to examine the louver performance under simulated lunar surface conditions.

The primary intended application of the technology presented here is to protect the spacecraft radiators from ionizing radiation, dust and excessive heat loss. However, key concepts and components of this technology can be extended to other space and terrestrial applications. For example, the Lotus coating (one of the components of our technology that provides passive dust mitigation) can be applied to protect optical/electrical components and solar panels on the moon, Mars and other planetary bodies, as well as to protect the solar panels on earth. Some of the features (like the protection from ionizing radiation and lunar night conditions) can be extended to shield other key components that are susceptible to degradation and irreversible failure such as batteries and fuel cells.

ACKNOWLEDGEMENTS

The authors would like to acknowledge the guidance and support provided by several NASA scientists and engineers including Dr. Tom Leimkuehler, Mr. Richard G. Schunk, Mr. Gary J. Rankin, Mr. Aaron A. Rodriguez, Mr. Todd Peters, Mr. Michael Reddington, and Mr. John Lauterbach. We would like to thank Mr. Dylan Nawn, Mr. Jeff Randall and Mr. Peter Neumann from Maxon for helping us with the selection of key components and the design of a space rated motor for our application. Finally, we would like to thank Prof. Mukul Shirvaikar and Prof. Masud Rana from the University of Texas at Tyler for helping with the motor control system design and the maturation of Lotus coating technology.

Trade names and trademarks are used in this report for identification only. Their usage does not constitute an official endorsement, either expressed or implied, by the National Aeronautics and Space Administration.

CONTACT

Vijay V. Devarakonda, PhD, Founder and CEO of Analytical Scientific Products and the Principle Investigator for this project can be reached at vijay@analyticalscientificproducts.com

REFERENCES

1. Cowan, D., "Actively Controlled Louver for Human Spacecraft Radiator Ultraviolet (UV), Dust, and Freeze Protection," 52nd International Conference on Environmental Systems, 16-20 July 2023, Calgary, Canada.
2. Sawyer, D.M., and Vette, J.I., "AP-8 Trapped Proton Environment for Solar Maximum and Solar Minimum," NASA Technical Memorandum TM-X-72605, pg. 87, December 1976.
3. Edwards, D.L., and Zwiener, J.M., "Radiation Induced Degradation of White Thermal Control Paints Z-93 and Z-93P," NASA Technical Memorandum 108518, October 1996.
4. Gilmore, D., Spacecraft Thermal Control Handbook, 2nd ed., The Aerospace Press, California, 2002, Chap. 6.
5. Gaier, J.R., Siamidis, J., et al., "The Effect of Simulated Lunar Dust on the Absorptivity, Emissivity, and Operating Temperature on AZ–93 and Ag/FEP Thermal Control Surfaces," NASA Technical Memorandum 215492, December 2008.
6. Sierra Nevada Corporation (SNC) Product Catalog 2015.
7. Sharon Straka, Kenneth O'Connor, Mark Hasegawa, Boxi Chen, Nathaniel Patrick Hawthorne, and Victoria Jane Peder Stotzer, "Superhydrophobic and dust mitigating coating", US Patent No. US 11,219,922 B1 January 11 2021.
8. Devarakonda, V.V. and M.D. Hogue, "Radiation, dust, and coolant freeze-out mitigation", SBIR Phase I Final Report, Solicitation Topic No. Z13.05, Contract No. 80NSSC24PB260, Report No. 4003-2025, February 2025.
9. NIST X-ray mass attenuation coefficients, https://physics.nist.gov/PhysRefData/XrayMassCoef/tab3.html

Trade names and trademarks are used in this report for identification only. Their usage does not constitute an official endorsement, either expressed or implied, by the National Aeronautics and Space Administration.